

Hindawi Publishing Corporation  
Journal of Catalysts  
Volume 2014, Article ID 413693, 8 pages  
<http://dx.doi.org/10.1155/2014/413693>



## Research Article

# Supported TiO<sub>2</sub> on Borosilicate Glass Plates for Efficient Photocatalytic Degradation of Fenamiphos

A. El Yadini,<sup>1</sup> H. Saufi,<sup>1</sup> P. S. M. Dunlop,<sup>2</sup> J. Anthony Byrne,<sup>2</sup>  
M. El Azzouzi,<sup>1</sup> and S. El Hajjaji<sup>1</sup>

<sup>1</sup> Laboratory of Spectroscopy, Molecular Modelisation, Material and Environment (LS3ME), Faculty of Sciences, University Med V-Agdal, Avenue Ibn Battouta, BP 1014, Agdal, Rabat, Morocco

<sup>2</sup> Nanotechnology and Integrated BioEngineering Centre, University of Ulster, Newtownabbey BT37 0QB, UK

Correspondence should be addressed to S. El Hajjaji; selhajjaji@hotmail.com

Received 4 September 2013; Revised 17 November 2013; Accepted 4 December 2013; Published 15 January 2014

Academic Editor: Raghunath V. Chaudhari

Copyright © 2014 A. El Yadini et al. This is an open access article distributed under the Creative Commons Attribution License, which permits unrestricted use, distribution, and reproduction in any medium, provided the original work is properly cited.

Supported titanium dioxide (TiO<sub>2</sub>) was investigated for the photodegradation of the insecticide fenamiphos in water. The photocatalyst was immobilised on borosilicate glass plates and the kinetics of degradation were studied in a stirred tank reactor under UV irradiation. Two types of TiO<sub>2</sub>, for example, Millennium PC500 (100% anatase) and Degussa P25 (80% anatase, 20% rutile), were used. Their activities have been based on the rates of insecticide disappearance. Experiments were investigated to evaluate the effect of pH and initial concentrations of fenamiphos as well as catalyst doses on the photocatalytic degradation of fenamiphos. Kinetic parameters were experimentally determined and an apparent first-order kinetic was observed. For photolysis process of fenamiphos, two photoproducts were identified and characterized using high performance liquid chromatography/mass spectrometry (HPLC/MS). The plausible mechanism of photolysis involved is the oxidation of sulfonamide group. In presence of photocatalyst TiO<sub>2</sub>, photodegradation was observed. Under identical conditions, Degussa P25 shows higher photocatalytic activity in regard to PC500 Millennium and complete degradation was observed after 180 min.

## 1. Introduction

In recent years, novel methods for water, soil, and air purification have been developed including chemical, electrochemical, and photochemical processes [1–4]. Indeed, photocatalytic degradation has been shown to be a promising technology for the treatment of water contaminated with organic and inorganic pollutants [1, 2]. Furthermore, photocatalysis has been reported to be effective for the degradation of persistent organic pollutants, such as pesticides, exhibiting chemical stability and resistance to natural biodegradation in water [5–11].

Using titanium dioxide as photocatalyst has been extensively investigated as an alternative physical-chemical process for decontamination of water pollution. Thus, the use of UV energy and TiO<sub>2</sub> as semiconductor either in suspension or immobilized on a thin layer can completely degrade or mineralize organic pollutants [12–17]. The Degussa P25

TiO<sub>2</sub>-type is a commercially available powder preparation and has emerged as the research standard in the field of photocatalysis. However, since the final filtration of titania powders in suspension for the release of cleaned water and the recovery of the catalysts is a tedious process, titania has been successfully deposited on different supports [18–24].

The pesticide selected here is fenamiphos (ethyl 4-methylthio-m-tolyl isopropylphosphoramidate) which is a typical organophosphate derivative and blocks the enzyme acetylcholinesterase in the target pests [25]. Generally, under environmental conditions, fenamiphos can be oxidized primarily to fenamiphos sulfoxide (FSO) followed by further oxidation to fenamiphos sulfone (FSO<sub>2</sub>) [26–28]. These oxidation products have nematocidal activity and toxicity similar to the parent compound, but they are much more mobile and persistent [27]. The soils of a neutral nature favour the accumulation of residues of this pesticide for a longer time which may contribute to groundwater pollution [29].

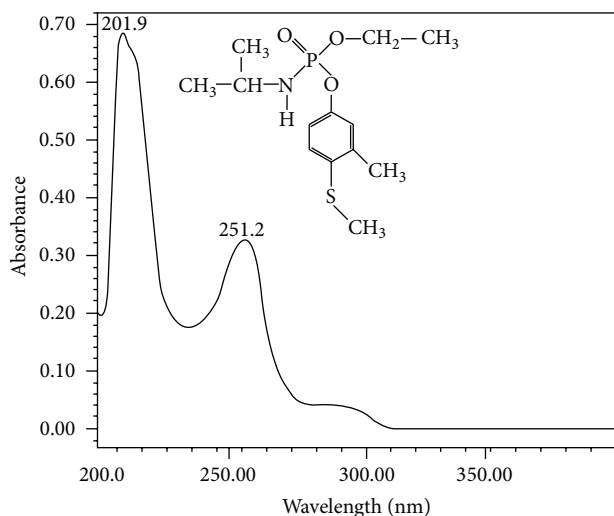


FIGURE 1: Chemical structure and absorbance spectrum of fenamiphos.

In this work, the original titania has been deposited on glass supports to be easily removed and recycled. The supporting substrates were borosilicate glass plates, transparent to UVA. The aim of this work is to study the photocatalytic degradation kinetics of fenamiphos by using these immobilised films of  $\text{TiO}_2$  in a stirred tank reactor. Both PC500 and P25 titanium dioxide were used as photocatalysts. The kinetics of degradation were determined at different pH and temperature values. In parallel, the effect of catalyst loading as immobilised films was studied to optimise the fenamiphos degradation.

## 2. Materials and Methods

**2.1. Chemicals.** Commercial fenamiphos with 99.5% purity was used. The absorbance spectrum of fenamiphos in aqueous solution is presented in Figure 1. All other chemicals were of analytical grade and were used without further purification. Solutions were prepared with high purity water. Also, all solvents used for HPLC analysis were of chromatography grade. A stock fenamiphos standard solution (1000 ppm in water) was prepared and an aliquot stock solution of 10 ppm was prepared.

**2.2. Immobilisation of  $\text{TiO}_2$ .**  $\text{TiO}_2$  was immobilised on borosilicate glass using spray coating technique [18, 23]. This is a simple and effective means to produce coatings on conducting and nonconducting supporting substrates. The process is not limited to substrate sizes and involves minimal equipment, operator training, and time. Two commercial preparations of  $\text{TiO}_2$  were used, that is, Degussa P25 (now Evonik Aeroxide P25) and Millennium PC500 (Table 1). The borosilicate glass plates (110 mm  $\times$  110 mm) were cleaned by sonication in hot 5% Decon 90/water solution, rinsed three times in distilled water, and then dried under a stream of nitrogen gas. The plates were then dried and weighed.  $\text{TiO}_2$  was spray coated using a 5%  $\text{TiO}_2$  methanol suspension using

a lab spray gun. The spray gun reservoir was shaken between applications to ensure that the catalyst powders remained in suspension. The plates were dried after each coating using an IR lamp. This procedure was repeated to produce plates with a range of  $\text{TiO}_2$  loadings. The plates were annealed in air at 673 K for 1 h to improve particle adhesion to the glass and particle-particle cohesion. Gravimetric analysis of the plates was used to determine the  $\text{TiO}_2$  loading. Glass plates with catalyst loadings ranging from 0.2 to 1.2  $\text{mg}/\text{cm}^2$  were produced for each photocatalyst. The borosilicate glass has a refractive index of 1.489 at  $\lambda = 365$  nm, which gives a corresponding loss due to reflection of a perpendicular beam of 3.8%.

**2.3. Photocatalytic Reactor.** A custom-built stirred tank photoreactor (STR), previously reported [18, 23, 24], was used in this study. The closed system consisted of a water-jacketed walled vessel reservoir and a stainless steel propeller in order to create a turbulent flow. Thus, good mass transfer behaviour is obtained based on a turbulent flow inside the reactor. This principle transports the organic pollutant towards the coated  $\text{TiO}_2$  plate and disperses oxygen from the headspace into the liquid. The  $\text{TiO}_2$  coated glass plate was illuminated from below by PL-S 9 W/10 UV-A fluorescent lamps (Philips) with a stable output between 350 and 400 nm (peak emission at 370 nm) or HPK 125 W mercury lamp with a high level of UV radiation (peak emission at 365 nm), positioned at a distance of 2.5 cm under the  $\text{TiO}_2$  glass plate. The light intensity entering the reactor was determined by potassium ferrioxalate actinometry technique. Oxygen (99.5%) or air was added to the headspace of the reactor at a constant flow of 900  $\text{cm}^3 \text{min}^{-1}$ . A schematic representation of the STR is given in Figure 2.

**2.4. Photocatalytic Experiments and Kinetics.** Prior to sample irradiation, the UVA lamps were allowed to stabilize for a period of 20 min. An aqueous solution of fenamiphos was added to the reactor and equilibrated in the dark at the studied pH and temperature. For photolysis experiments (UVA only), a borosilicate glass plate was used without the  $\text{TiO}_2$  coating. Dark control experiments were also carried out to investigate adsorption of fenamiphos to the  $\text{TiO}_2$  films. Degradation of micropollutants in the environment is mainly driven by different environmental forces such as biotic degradation. Thus, temperature is considered among the most factors that can influence the degradation rates of micropollutants by increasing the biotic and/or abiotic reactions of these compounds. It is well known that the degree of the effect of the temperature on the kinetic degradation of the pesticides depends on (i) their chemical structures types and (ii) the pH of the medium [30, 31]. The kinetic experiments were performed by following the disappearance of herbicide by means of HPLC at the pH 5.8 and the temperature of 25°C. All solutions were stirred and samples from considered solutions were taken at regular time intervals and then analyzed directly without preconcentration by HPLC. Other tests were made on the degradation kinetics using natural sunlight. The samples were irradiated continuously

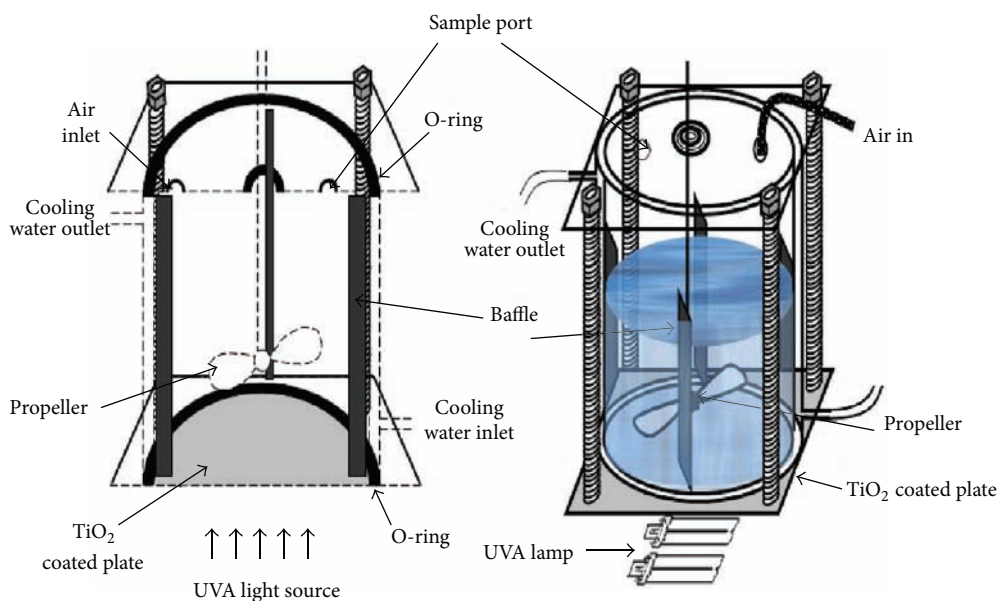


FIGURE 2: Schematic representation of a stirred tank reactor.

TABLE 1: Proprieties of TiO<sub>2</sub> crystallites used.

Product	Supplier	Composition	Crystallites size (nm)	Surface area (m <sup>2</sup> /g)
PC500	Millennium	Anatase	5–10	>300
P25	Degussa	Anatase/rutile (4/1)	25–30	55 ± 15

for 2 h under the effect of light lamps. All experiments were performed in duplicate.

## 2.5. Analytical Methods

**2.5.1. High Performance Liquid Chromatography (HPLC).** The analysis was performed using an HPLC system. The instrument used for the photochemical study was a GBC equipped with a detector and a GBC LC 1150 pump. A column Agilent Zorbax SB-C18 (4.6 × 250 mm) was used for analysis. The other HPLC conditions are as follows: (i) mobile phase was a mixture of water (30%) and methanol (70%), (ii) wave length was 249 nm, and (iii) flow rate was 1 mL/min.

**2.5.2. Total Organic Carbon Analysis (TOC).** TOC analysis was carried out using a Shimadzu 5000A TOC analyser. This system uses a Pt furnace at 650 °C with detection of carbon by IR-CO<sub>2</sub> analysis. Inorganic carbon (IC) is measured by CO<sub>2</sub> analysis following acidification. Total carbon (TC) – IC = TOC.

## 3. Results and Discussion

### 3.1. Photolysis of Fenamiphos

**3.1.1. Kinetics.** The direct irradiation of a solution containing 32.9 μM (10 ppm) of fenamiphos was conducted over a period of 2 hours or 3 hours using UV light, with regular sampling every 10 minutes. Analysis of solutions by HPLC-UV shows a

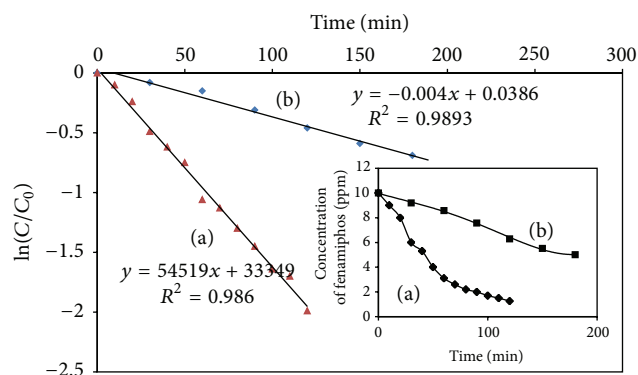


FIGURE 3: Semilog plots of  $\ln(C/C_0)$  over time were plotted for fenamiphos photolysis, using HPLC 125 W Phillips lamp (a) and PL-S 9 W/10 Phillips lamp (b).

steady decrease in the concentration of fenamiphos versus the time of irradiation (Figure 3). The photolysis of fenamiphos in water was modeled with a first-order kinetic. The evolution of  $\ln(C/C_0)$  versus time is shown in Figure 3. The disappearance of fenamiphos follows apparent first-order kinetics and the rate constant is presented in Table 2. HPLC/MS analysis was carried out to follow the main intermediates resulted from the photolytic process of fenamiphos.

**3.1.2. Identification of Photoproducts.** Figure 4 shows HPLC chromatograms illustrating the disappearance of fenamiphos

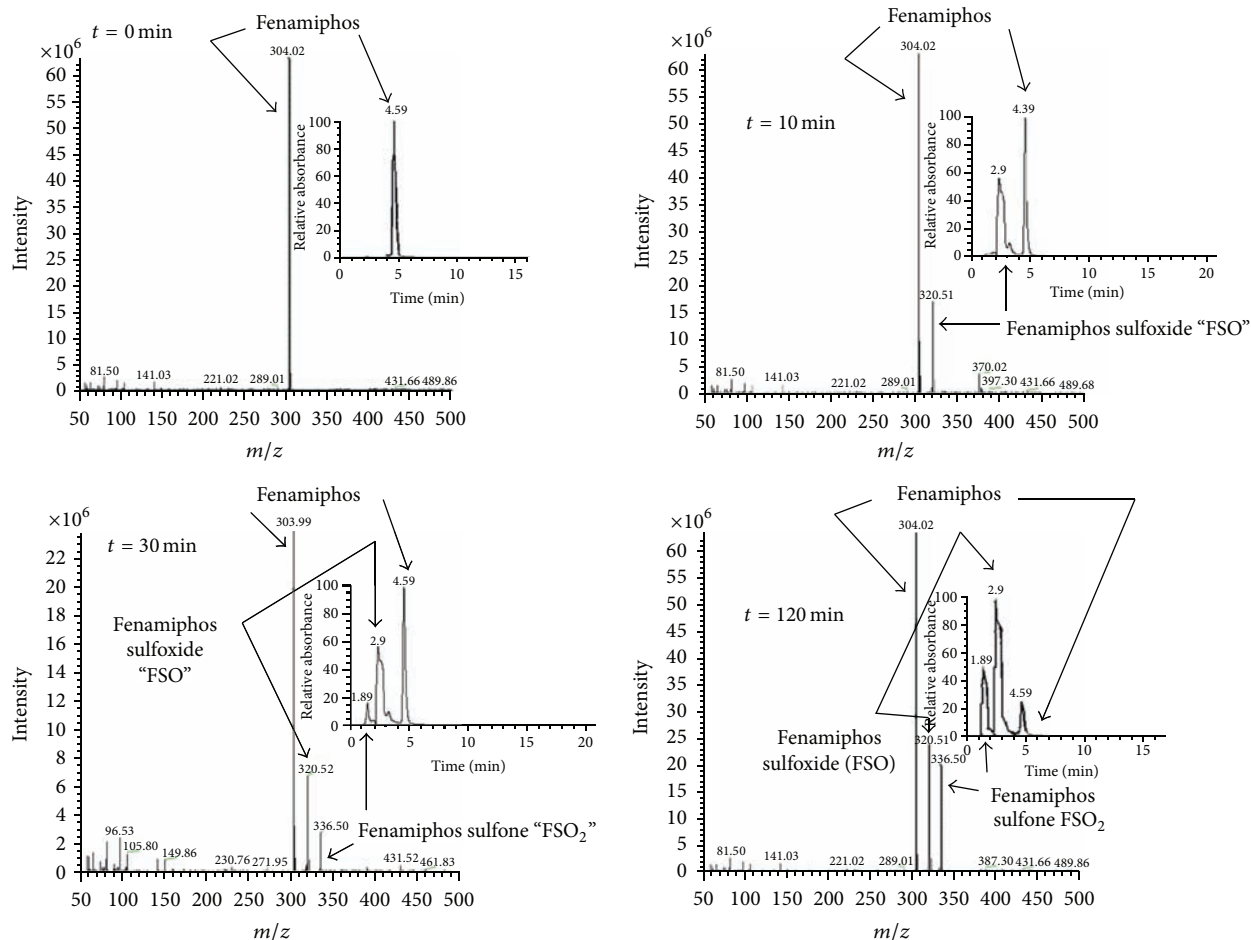


FIGURE 4: HPLC spectrum for times 0, 10, 30, and 120 min of photocatalytic treatment, showing decrease of fenamiphos and increase of the formation of intermediates.

TABLE 2: Rate constant ( $k$ ) and half-life ( $t_{1/2}$ ) of transformation of fenamiphos during photolysis process using HPLK 125 W Phillips lamp (a) and PL-S 9 W/10 Phillips lamp (b).

Lamp	Kinetics parameters			$R^2$
HPLK 125 W	Kinetic constant $k$ ( $10^{-3} \text{ min}^{-1}$ )		14.47	0.986
HPLK 125 W	Half-life $t_{1/2}$ (min)		48	
PL-S 9 W/10	Kinetic constant $k$ ( $10^{-3} \text{ min}^{-1}$ )		4.11	0.9893
PL-S 9 W/10	Half-life $t_{1/2}$ (min)		168.6	

over irradiation time. According to different irradiation time, the peak of fenamiphos decreases with the formation of two intermediates products at retention times 2.9 and 1.89 minutes, respectively (Table 3).

Analysis by HPLC-MS allowed us to identify the byproducts of photolysis with  $m/z = 320.51$  and  $m/z = 336.50$ , which can be assigned, respectively, to fenamiphos sulfoxide (FSO) and fenamiphos sulfone  $\text{FSO}_2$  (Figure 4).

The evolution of fenamiphos and its intermediate as a function of the irradiation time is shown in Figure 5. We can clearly observe the appearance of two intermediates products, 10 and 30 minutes, after the irradiation by UV lamps. The transformation of fenamiphos corresponds to the transformation of fenamiphos to fenamiphos sulfoxide (FSO) which

occurs rapidly and continues during the irradiation (2 hours). After 20 minutes, fenamiphos sulfoxide (FSO) was oxidized on fenamiphos sulfone ( $\text{FSO}_2$ ) and the concentration of FSO decreases during the first 30 minutes, but the rate of fenamiphos transformation on FSO is more important than the oxidation of FSO on  $\text{FSO}_2$  as shown in Figure 5 and Table 3.

On the basis of the identified photoproducts and the sequence of their formation during the experiment, we would suggest that the photolysis of fenamiphos in water proceeds via oxidation pathway [32, 33]. Fenamiphos oxidizes in fenamiphos sulfoxide (FSO) by the effect of light and it oxidizes to fenamiphos sulfone ( $\text{FSO}_2$ ). No other products were observed like the phenol derivative which corresponds

TABLE 3: Retention time and  $m/z$  values of phototransformation products of fenamiphos after 120 minutes of irradiation time.

	Fenamiphos	Fenamiphos sulfoxide (FSO)	Fenamiphos sulfone (FSO <sub>2</sub> )
Masse ( $m/z$ )	304.02	320.51	336.50
Retention time (min)	4.59	2.9	1.89

TABLE 4: Calculated pseudofirst-order rate constants and half-life for fenamiphos photocatalytic degradation using supported catalysts TiO<sub>2</sub> P25 and TiO<sub>2</sub> PC500.

	$k$ (min <sup>-1</sup> )	$t_{1/2}$ (min)
P25	0.0183	37.8
PC500	0.0122	56.8

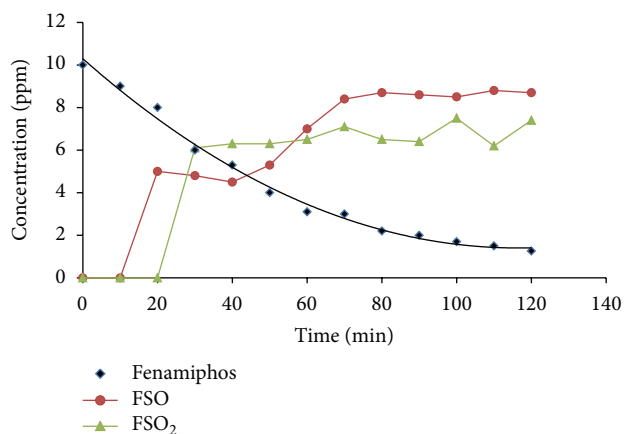


FIGURE 5: The evolution of fenamiphos and its intermediate as a function of the irradiation time.

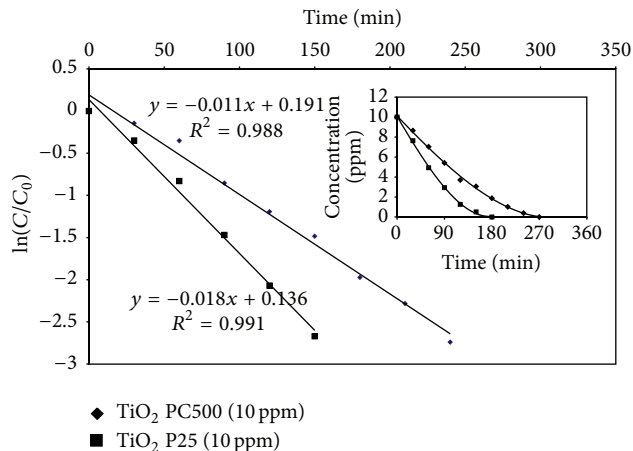
to the photohydrolysis of fenamiphos as generally observed for the photodegradation of fenamiphos in soil [11].

### 3.2. Photocatalysis of Fenamiphos

**3.2.1. Nature of TiO<sub>2</sub> Effect.** Our study started on the use of P25 as immobilised photocatalyst. Figure 6 shows that the parent pesticide is completely degraded following 180 min of photocatalytic treatment in the reactor. It is interesting to note that, as this reactor was designed to determinate the intrinsic kinetics of photocatalytic degradation, the data obtained are useful for the development of large-scale photocatalytic reactions for water purification. Therefore, the time taken for pesticide degradation should not be used for comparison but rather the rate in terms of moles degraded per area of illuminated catalyst.

As shown in Figure 6, the photocatalytic degradation of fenamiphos follows a pseudo first-order kinetic by a good linear correlation between concentrations and time. The data of the constant kinetic and the half-life time are given in Table 4.

Then, we turned our attention on the use of PC500 as photocatalytic agent (Figure 6). Also, the degradation follows pseudofirst-order kinetics (Figure 6), but the rate is much lower, taking up to 270 min to reach complete destruction

FIGURE 6: Semilog plots of  $\ln(C/C_0)$  over time were plotted for fenamiphos photocatalysis in presence of different types of TiO<sub>2</sub> (1 mg/cm<sup>2</sup>, initial pH 5.8).

of the parent compound, in comparison with P25 showing a complete degradation after 180 min.

The first-order rate constant “ $k$ ” and the half-life ( $t_{1/2}$ ) are determined (Table 4). For the two TiO<sub>2</sub> types, the disappearance of fenamiphos follows apparent first-order kinetics. The rate of photocatalysis and the half-life varied with respect to the type of TiO<sub>2</sub>, being more rapid with P25 than with PC500. As reported by other authors, in the majority of studies, which have compared TiO<sub>2</sub> catalysts like PC500 to Degussa P25, the last one present the higher efficiency. Degussa P25 contains a small rutile core surrounded by anatase crystallites. According to this structure, the high photocatalytic efficiency has been attributed to catalytic “hot spots” at the intersection of the two phases due to the unique surface chemistry [18].

**3.2.2. Effect of Catalyst Loading.** For both of the photocatalysts used, further work was undertaken to determine the effect of photocatalyst loading on the rate of degradation of fenamiphos. The rate of degradation was determined using different catalyst loadings. The selected catalyst loadings are as follows: 0.2; 0.4; 0.6; 0.8; 1.0; and 1.2 mg cm<sup>-2</sup>. The initial concentration of fenamiphos was 10 ppm.

As shown in Table 4, the rate of degradation increased by increasing the catalyst loading up to around 1 mg cm<sup>-2</sup>. A decrease in the degradation rate was observed with a catalyst loading above. Strongly, these results correlate with previous results concerning the degradation of atrazine in the same system, where the initial rate increased with TiO<sub>2</sub> loading up to an optimum of 1.10 mg cm<sup>-2</sup> [24]. The effect of catalyst loading was also determined for PC500 and the results are presented in Table 5. Also, it was found that the optimum

TABLE 5: TOC values of fenamiphos degradation with regard to the amount of supported TiO<sub>2</sub> for irradiation time of 180 min.

Amount of TiO <sub>2</sub> P25 (mg/cm <sup>2</sup> )	0.2	0.4	0.6	0.8	<b>1</b>	1.2
TOC [%]	14.75	43.07	48.09	53.26	<b>59.84</b>	61.47
<i>k</i> (min <sup>-1</sup> )	0.0132	0.0169	0.0213	0.0256	<b>0.0303</b>	0.0286
Amount of TiO <sub>2</sub> PC500 (mg/cm <sup>2</sup> )	0.2	0.4	0.6	0.8	<b>1</b>	1.2
TOC [%]	21.93	25.28	29.46	36.15	<b>41.25</b>	36.22
<i>k</i> (min <sup>-1</sup> )	0.0097	0.0104	0.0137	0.0157	<b>0.0226</b>	0.0184

The bold values are the corresponding values to 1 mg·cm<sup>2</sup> because there are the best values obtained.

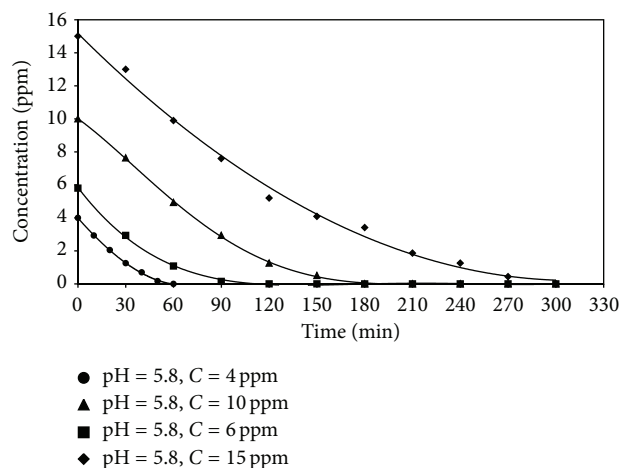


FIGURE 7: Disappearance of fenamiphos over time was plotted for each initial concentration of fenamiphos studied using supported TiO<sub>2</sub> P25 (1 mg/cm<sup>2</sup>, pH = 5.8).

catalyst loading was around 1 mg cm<sup>-2</sup> and, above this loading, low increase in the rate of degradation was observed. For higher quantities of catalyst, the reaction kinetic decreases because of the saturation of photons absorption [11, 18, 23, 24].

**3.2.3. Effect of Initial Concentration of Fenamiphos.** Figure 7 shows the kinetic curve of degradation of fenamiphos in the presence of P25 catalyst supported on glass with different concentrations of fenamiphos (4, 6, 10, and 15 ppm); the initial pH was of 5.8. Plots of disappearance of fenamiphos versus time for each concentration (Figure 7) suggested that the kinetics appeared to deviate from first-order kinetics.

According to the obtained results, the rate of degradation is relatively constant with changing initial concentration suggesting that we are operating in the high end of concentrations assuming a Langmuir-Hinshelwood kinetic model, widely observed for the photocatalytic degradation of organic pollutants on TiO<sub>2</sub> [11].

**3.2.4. Evaluation of TOC.** Finally, photocatalysis is a degradative process; the evaluation of the total organic carbon as a global measurement of the concentration of the organic intermediates produced during the degradation has been evaluated. Figure 8 shows the decrease of TOC versus time for the photocatalytic degradation of fenamiphos on P25.

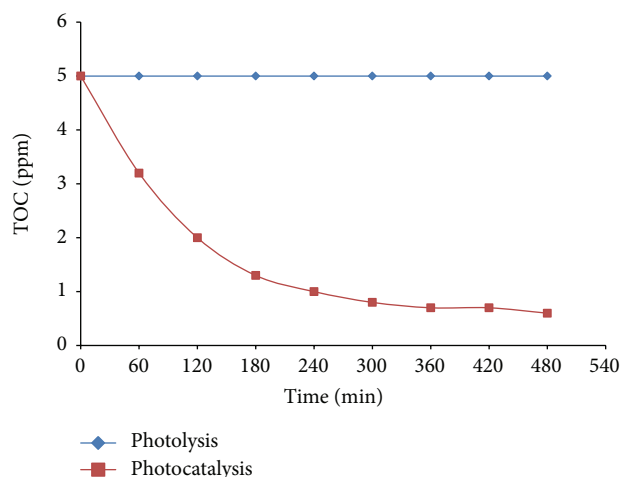


FIGURE 8: TOC versus time for the degradation of fenamiphos (10 ppm) on supported TiO<sub>2</sub> P25 (1 mg/cm<sup>2</sup>).

## 4. Conclusion

The photocatalytic degradation of the pesticide fenamiphos was studied in a custom-built stirred tank photoreactor using two commercial preparations of TiO<sub>2</sub>: Degussa P25 and Millennium PC500. The catalysts were immobilised on borosilicate glass at different loadings. It was found that the degradation of fenamiphos followed pseudofirst-order kinetics for both catalysts studied. Also, it was determined that the optimum catalyst loading for both preparations was around 1 mg cm<sup>-2</sup>. The degradation rate was also studied as a function of initial concentration of fenamiphos and it was found that the initial rate remained relatively constant in the range of concentrations studied, suggesting that we were operating in the high end of concentrations resulting in an observed zero-order kinetic, as predicted by a Langmuir-Hinshelwood kinetic model. Furthermore, when the initial solution pH was below the PZC of TiO<sub>2</sub>, there was an increase in the rate of degradation as compared to neutral pH and in slightly alkaline conditions. Finally, the removal of TOC indicates the mineralisation of fenamiphos. These results show that immobilised films of TiO<sub>2</sub> are able to degrade the pesticide fenamiphos and may find application in the remediation of water contaminated with pesticide residues where efficient reactor design is employed.

## Conflict of Interests

The authors declare that there is no conflict of interests regarding the publication of this paper.

## Acknowledgment

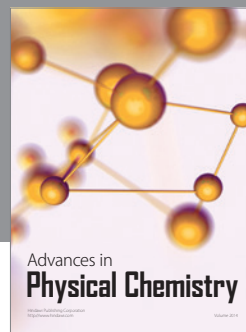
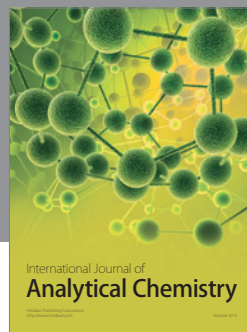
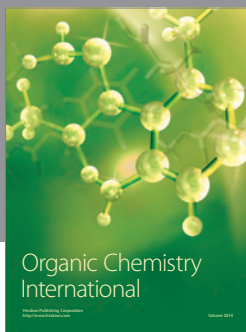
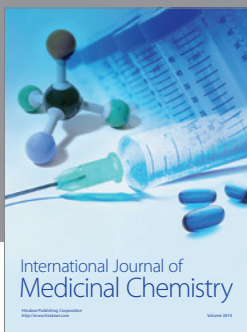
The authors wish to acknowledge NATO Science for Peace and Security for funding this research under Grant no. ESP.MD.CLG 983344.

## References

- [1] G. Centi and S. Perathoner, "Remediation of water contamination using catalytic technologies," *Applied Catalysis B*, vol. 41, no. 1-2, pp. 15–29, 2003.
- [2] S. Chiron, A. Fernandez-Alba, A. Rodriguez, and E. Garcia-Calvo, "Pesticide chemical oxidation: state-of-the-art," *Water Research*, vol. 34, no. 2, pp. 366–377, 2000.
- [3] H. D. Burrows, L. M. Canle, J. A. Santaballa, and S. Steenken, "Reaction pathways and mechanisms of photodegradation of pesticides," *Journal of Photochemistry and Photobiology B*, vol. 67, no. 2, pp. 71–108, 2002.
- [4] L. Tajeddine, M. Nemmaoui, H. Mountacer, A. Dahchour, and M. Sarakha, "Photodegradation of fenamiphos on the surface of clays and soils," *Environmental Chemistry Letters*, vol. 8, no. 2, pp. 123–128, 2010.
- [5] D. F. Ollis, "Contaminant degradation in water," *Environmental Science & Technology*, vol. 19, no. 6, pp. 480–484, 1985.
- [6] R. W. Matthews, "Solar-electric water purification using photocatalytic oxidation with TiO<sub>2</sub> as a stationary phase," *Solar Energy*, vol. 38, no. 6, pp. 405–413, 1987.
- [7] M. Schiavello, *Photocatalysis and Environment—Trends and Applications*, Kluwer, Dordrecht, The Netherlands, 1988.
- [8] N. Serpone and E. Pelizzetti, *Photocatalysis, Fundamentals and Applications*, Wiley, New York, NY, USA, 1989.
- [9] J. M. Herrmann, "Water treatment by heterogeneous photocatalysis," in *Environmental Catalysis*, F. J. J. G. Janssen and R. A. van Santen, Eds., pp. 171–194, Imperial Press, 1999.
- [10] J. M. Herrmann, "Solar detoxification of wastewaters," in *Industrial Applications of Solar Chemistry*, D. Martinez, Ed., pp. 31–63, CIEMAT, Madrid, Spain, 2000.
- [11] M. R. Hoffmann, S. T. Martin, W. Choi, and D. W. Bahnemann, "Environmental applications of semiconductor photocatalysis," *Chemical Reviews*, vol. 95, no. 1, pp. 69–96, 1995.
- [12] K. Djebbar and T. Sehili, "Kinetics of heterogeneous photocatalytic decomposition of 2,4-dichlorophenoxyacetic acid over titanium dioxide and zinc oxide in aqueous solution," *Pesticide Science*, vol. 54, no. 3, pp. 269–276, 1998.
- [13] M. E. Madani, C. Guillard, N. Pérol et al., "Photocatalytic degradation of diuron in aqueous solution in presence of two industrial titania catalysts, either as suspended powders or deposited on flexible industrial photoresistant papers," *Applied Catalysis B*, vol. 65, no. 1-2, pp. 70–76, 2006.
- [14] J. C. Garcia and K. Takashima, "Photocatalytic degradation of imazaquin in an aqueous suspension of titanium dioxide," *Journal of Photochemistry and Photobiology A*, vol. 155, no. 1-3, pp. 215–222, 2003.
- [15] C. Guillard, J. Disdier, C. Monnet et al., "Solar efficiency of a new deposited titania photocatalyst: chlorophenol, pesticide and dye removal applications," *Applied Catalysis B*, vol. 46, no. 2, pp. 319–332, 2003.
- [16] M. Harir, A. Gaspar, B. Kanawati et al., "Photocatalytic reactions of imazamox at TiO<sub>2</sub>, H<sub>2</sub>O<sub>2</sub> and TiO<sub>2</sub>/H<sub>2</sub>O<sub>2</sub> in water interfaces: kinetic and photoproducts study," *Applied Catalysis B*, vol. 84, no. 3-4, pp. 524–532, 2008.
- [17] A. E. Kinkennon, D. B. Green, and B. Hutchinson, "The use of simulated or concentrated natural solar radiation for the TiO<sub>2</sub>-mediated photodecomposition of Basagran, Diquat, and Diuron," *Chemosphere*, vol. 31, no. 7, pp. 3663–3671, 1995.
- [18] P. S. M. Dunlop, A. Galdi, T. A. McMurray, J. W. J. Hamilton, L. Rizzo, and J. A. Byrne, "Comparison of photocatalytic activities of commercial titanium dioxide powders immobilised on glass substrates," *Journal of Advanced Oxidation Technologies*, vol. 13, no. 1, pp. 99–106, 2010.
- [19] R. L. Pozzo, M. A. Baltanás, and A. E. Cassano, "Supported titanium oxide as photocatalyst in water decontamination: state of the art," *Catalysis Today*, vol. 39, no. 3, pp. 219–231, 1997.
- [20] M. El Madani, M. Harir, A. Zrineh, and M. El Azzouzi, "Photodegradation of imazethapyr herbicide by using slurry and supported TiO<sub>2</sub>: efficiency comparison," *Arabian Journal of Chemistry*, 2011.
- [21] C. Guillard, J. Disdier, J. M. Herrmann et al., "Solar efficiency of a photocatalytic nonwoven: dye removal applications," in *Serie Ponencias*, pp. 59–66, CIEMAT, Madrid, Spain, 2002.
- [22] C. Sarantopoulos, E. Puzenat, C. Guillard, J. M. Herrmann, A. N. Gleizes, and F. Maury, "Microfibrillar TiO<sub>2</sub> supported photocatalysts prepared by metal-organic chemical vapor infiltration for indoor air and waste water purification," *Applied Catalysis B*, vol. 91, no. 1-2, pp. 225–233, 2009.
- [23] T. A. McMurray, J. A. Byrne, P. S. M. Dunlop, J. G. M. Winkelman, B. R. Eggins, and E. T. McAdams, "Intrinsic kinetics of photocatalytic oxidation of formic and oxalic acid on immobilised TiO<sub>2</sub> films," *Applied Catalysis A*, vol. 262, no. 1, pp. 105–110, 2004.
- [24] T. A. McMurray, P. S. M. Dunlop, and J. A. Byrne, "The photocatalytic degradation of atrazine on nanoparticulate TiO<sub>2</sub> films," *Journal of Photochemistry and Photobiology A*, vol. 182, no. 1, pp. 43–51, 2006.
- [25] H. Kidd and D. R. James, *The Agrochemicals Handbook*, Royal Society of Chemistry Information Services, Cambridge, UK, 3rd edition, 1991.
- [26] L. T. Ou, J. E. Thomas, and D. W. Dickson, "Degradation of fenamiphos in soil with a history of continuous fenamiphos applications," *Soil Science Society of America Journal*, vol. 58, no. 4, pp. 1139–1147, 1994.
- [27] T. Cáceres, M. Megharaj, and R. Naidu, "Toxicity of fenamiphos and its metabolites to the cladoceran *Daphnia carinata*: the influence of microbial degradation in natural waters," *Chemosphere*, vol. 66, no. 7, pp. 1264–1269, 2007.
- [28] S. El Hajjaji, A. El Yadini, A. Dahchour, M. El Azzouzi, A. Zouaou, and M. M'Rabet, "Phototransformation of organophosphorus pesticide in aqueous solution under irradiation light," *Environmental Science*, vol. 5, no. 6, 2010.
- [29] P. D. Franzmann, L. R. Zappia, A. L. Tilbury, B. M. Patterson, G. B. Davis, and R. T. Mandelbaum, "Bioaugmentation of atrazine and fenamiphos impacted groundwater: laboratory evaluation," *Bioremediation Journal*, vol. 4, no. 3, pp. 237–248, 2000.
- [30] A. Chnirheb, M. Harir, B. Kanawati et al., "Hydrolysis of mefenpyr-diethyl: an analytical and DFT investigation," *Analytical and Bioanalytical Chemistry*, vol. 398, no. 5, pp. 2325–2334, 2010.

- [31] S. B. Lartiges and P. P. Garrigues, "Degradation kinetics of organophosphorus and organonitrogen pesticides in different waters under various environmental conditions," *Environmental Science and Technology*, vol. 29, no. 5, pp. 1246–1254, 1995.
- [32] R. S. Kookana, C. Phang, and L. A. G. Aylmore, "Transformation and degradation of fenamiphos nematicide and its metabolites in soils," *Australian Journal of Soil Research*, vol. 35, no. 4, pp. 753–761, 1997.
- [33] P. Dureja, "Photolysis of benfuracarb," *Toxicological and Environmental Chemistry*, vol. 28, no. 4, pp. 189–244, 1990.





**Hindawi**

Submit your manuscripts at  
<http://www.hindawi.com>

